Cellular Microbiology (2001) **3**(6), 427–437

Low iron availability modulates the course of *Chlamydia pneumoniae* infection

Hesham M. Al-Younes,[1] Thomas Rudel,[1] Volker Brinkmann,[2] Agnes J. Szczepek[1] and Thomas F. Meyer[1]*

[1]*Department of Molecular Biology and*
[2]*Central Microscopy Unit, Max Planck Institute for Infection Biology, Schumannstrasse 21/22, D-10117 Berlin, Germany.*

Summary

Chlamydiae are obligate intracellular bacteria residing exclusively in host cell vesicles termed inclusions. We have investigated the effects of deferoxamine mesylate (DAM)-induced iron deficiency on the growth of *Chlamydia pneumoniae and Chlamydia trachomatis* serovar L2. In epithelial cells subjected to iron starvation and infected with either *C. pneumoniae* or *C. trachomatis* L2, small inclusions were formed, and the infectivity of chlamydial progeny was impaired. Moreover, for *C. trachomatis* L2, we observed a delay in homotypic fusion of inclusions. The inhibitory effects of DAM were reversed by adding exogenous iron-saturated transferrin, which restored the production of infectious chlamydiae. Electron microscopy examination of iron-deprived specimens revealed that the small inclusions contained reduced numbers of *C. pneumoniae* that were mostly reticulate bodies. We have previously reported specific accumulation of transferrin receptors (TfRs) around *C. pneumoniae* inclusions within cells grown under normal conditions. Using confocal and electron microscopy, we show here a remarkable increase in the amount of TfRs surrounding the inclusions in iron-starved cultures. It has been shown that iron is an essential factor in the growth and survival of *C. trachomatis.* Here, we postulate that, for *C. pneumoniae* also, iron is an indispensable element and that *Chlamydia* may use iron transport pathways of the host by attracting TfR to the phagosome.

Introduction

Chlamydia spp. represent obligate intracellular bacteria that multiply within host cells in a membrane-bound inclusion. The genus *Chlamydia* has a unique biphasic developmental cycle with morphologically and functionally distinct forms: the infectious, metabolically inactive elementary body (EB) and the non-infectious, metabolically active reticulate body (RB). Upon entry into a host cell, EBs reorganize within the inclusion into RBs that multiply by binary fission. The RBs finally differentiate back into EBs that are released after lysis of the inclusion membrane and the host cell, starting another cycle of infection (Peeling and Brunham, 1996).

Chlamydia trachomatis causes trachoma and human genital tract infections (Peeling and Brunham, 1996). The recently recognized *Chlamydia pneumoniae* has been implicated in a significant number of human respiratory diseases, including pneumonia, bronchitis, asthma, sinusitis and pharyngitis (Grayston *et al*., 1990). Other studies have reported a link between *C. pneumoniae* infections and coronary heart diseases (Saikku, 2000). The majority of published evidence associates persistent *C. pneumoniae* infections with atherogenesis by seroepidemiological studies, demonstration of pathogen in atheromas by polymerase chain reaction (PCR), immunocytochemistry, *in situ* hybridization, electron microscopy and by the recovery of bacteria in tissue culture (Ramirez, 1996). Furthermore, respiratory inoculation of *C. pneumoniae* in experimental animal models induced or accelerated the formation of atherosclerotic lesions (de Boer *et al*., 2000).

Iron is an essential metal involved in vital cell functions, such as electron transport and DNA synthesis, and serves as a cofactor for many enzymes (Ponka, 1999). The current literature supports the view that iron is transferred to and used by *Chlamydia*. Exposure of *C. trachomatis*-infected cell cultures to transferrin (Tf) radiolabelled with ^{55}Fe resulted in the transfer of the iron isotope to EBs, demonstrating the ability of the pathogen to obtain iron from Tf (Scidmore and Hackstadt, 1995). Genes encoding homologues of enzymes and proteins regulated by iron were found in chlamydial genomes (http://www.stdgen.lanl.gov), for example ribonucleotide reductase (gene ID: CPn0984, CPn0985, CT827 and CT828), ferredoxin IV (CPn0364 and CT059), ferrochelatase (CPn0603 and CT485), chelated metal transport system membrane protein (CPn0543 and CT417) and SpoOJ regulator (CPn0805 and CT582). The abnormal growth and disrupted developmental cycle of *C. trachomatis* induced upon iron starvation

Received 26 June, 2000; revised 3 January, 2001; accepted 19 January, 2001. *For correspondence. E-mail meyer@mpiib-berlin.mpg.de; Tel. (+49) 30 284 60 402; Fax (+49) 30 284 60 401.

that can be counteracted by the addition of iron-loaded Tf (Raulston, 1997) strongly suggest a central role for this factor in some chlamydial metabolic functions, especially ribonucleotide reductase-dependent DNA synthesis and subsequent bacterial cell division.

Uptake of iron into host cells is mediated by Tf, a serum glycoprotein that has two binding sites for ferric iron (Fe^{3+}). After attachment to the cell surface transferrin receptor (TfR, CD71), the iron-saturated complex is internalized into an early endosomal compartment. Upon acidification, iron is released from Tf and enters the labile (free) iron pool before being used for metabolic activities or bound by iron storage compounds such as ferritin (Ponka, 1999; Ponka and Lok, 1999). The free intracellular iron can be removed by cell-permeable iron chelators such as deferoxamine mesylate (DAM), which removes only free iron and not iron bound to host iron-chelating proteins (Jacobs, 1977; Cabantchik *et al*., 1999). The effects of iron deprivation on *Chlamydia psittaci* (Murray *et al*., 1991), *C. trachomatis* serovar E (Raulston, 1997) and other intracellular pathogens have been analysed previously *in vitro* and/or *in vivo* using DAM at concentrations ranging from 15 μM to 2.5 mM. Most of these reports concluded that intracellular bacteria [*Coxiella burnetii* (Howe and Mallavia, 1999), *Francisella tularensis* LVS (Fortier *et al*., 1995), *Legionella pneumophila* (Byrd and Horwitz, 1989) and *Ehrlichia chaffeensis* (Barnewall and Rikihisa, 1994)] derive iron needed for optimal growth and virulence from the labile iron pool of the host cell. A significant role for iron in the biology of *C. pneumoniae* was stressed by Sullivan and Weinberg (1999), who postulated that growth and the establishment of chronic infection by *C. pneumoniae* in coronary arteries can be achieved only if excess iron is present.

We have demonstrated previously the presence of TfR adjacent to *C. pneumoniae* inclusions (Al-Younes *et al*., 1999), a phenomenon also shown for other chlamydial species (Scidmore *et al*., 1996; Van Ooij *et al*., 1997; Hackstadt *et al*., 1998). Other groups have suggested that endosomes could be used by chlamydiae to acquire nutrients from the host cell (Van Ooij *et al*., 1997). Accordingly, we speculated that the accumulation of TfR to the chlamydial inclusions could reflect part of the process of iron delivery to *C. pneumoniae.*

In this study, we have investigated the role of iron in the growth and pathogenesis of *C. pneumoniae* and compared it with that of the lymphogranuloma venereum (LGV) serovar L2 of *C. trachomatis* (*C. trachomatis* L2). Using immunofluorescence and electron microscopy, we examined changes in the appearance of individual bacteria and chlamydial inclusions that were induced by limited accessibility to iron. Alteration of infectivity for iron-starved chlamydial progeny was also studied.

Results

Effects of iron chelation on C. trachomatis *L2 growth*

The response of *C. trachomatis* L2 to intracellular iron depletion, generated in HEp-2 cells by DAM, was monitored by microscopy and infectivity assays. The iron chelator concentrations ranged from 5 to 100 μM, and the host cells were infected for a maximum of 48 h. These concentrations did not affect the viability of host cells, as determined by Trypan blue uptake and Mito-Tracker staining (data not shown). Exposure of cells to either 5 or 10 μM DAM resulted in the formation of inclusions of similar size to those in the untreated controls (data not shown). However, treatment of cells with 15, 30, 50 or 100 μM DAM caused the production of smaller inclusions compared with those in untreated infected control cells (data not shown). The decrease in inclusion size in the treated cultures was dose dependent.

Another effect of iron starvation was an alteration in the characteristic homotypic fusion of *C. trachomatis* L2 inclusions. At the beginning of infection, *C. trachomatis* EBs are confined in multiple individual vacuoles that subsequently fuse, generating a single large inclusion (Blyth and Taverne, 1972). The fusion was found to be initiated by 10 h after infection and completed 25 h after infection (Matsumoto *et al*., 1991; Van Ooij *et al*., 1998; Hackstadt *et al*., 1999). In our experimental system, when cell cultures infected with *C. trachomatis* L2 and exposed to DAM were examined with light and fluorescence microscopy 20 h after infection, we observed the frequent presence of cells with multiple inclusions (Fig. 1C and D) compared with iron-replete infected cultures (Fig. 1A and B). To test quantitatively for the effect of iron starvation on the homotypic inclusion fusion, monolayers grown under either iron-sufficient or iron-limited conditions and infected at a multiplicity of infection (MOI) of 15 for 20 or 35 h were immunostained for chlamydiae, and the infected cells containing multiple inclusions were carefully enumerated. DAM-exposed monolayers infected for 20 h contained considerably higher numbers of cells with multiple inclusions compared with the untreated infected control cell cultures (Fig. 2, open bars). The number of inclusions in one cell was usually two to four, but some cells contained up to nine. The percentage of cells with multiple inclusions decreased to $< 10\%$ when cultures were examined 35 h after infection (Fig. 2, closed bars), indicating that the inclusions fused later in the developmental cycle. Although the number of cells with multiple bacterial inclusions increased as the MOI increased, the absolute number of inclusions per cell did not correlate significantly with the MOI and remained mostly two to four (data not shown). Lack of inclusion fusion at 20 h was also detected in HeLa cells (data not shown), indicating that this phenomenon is not cell line specific.

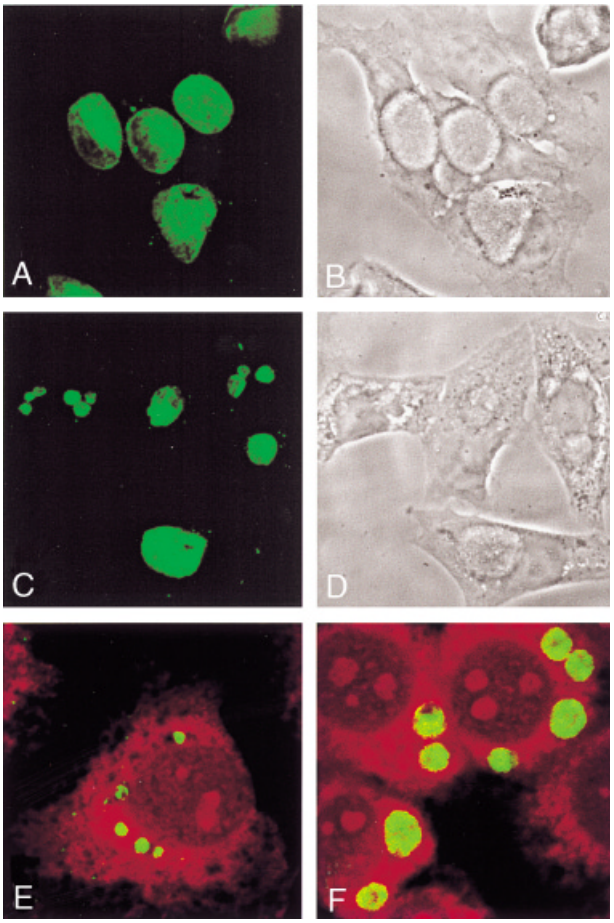

Fig. 1. Iron starvation modifies the size and some properties of chlamydial inclusions. Formation of small *C. trachomatis* L2 inclusions (green) in cells exposed to 50 μM DAM (C) compared with those in the control infected cells (A) 20 h after infection. Moreover, iron removal delayed the characteristic fusion between *C. trachomatis* L2 inclusions (C).
(B) and (D) are phase-contrast images of (A) and (C) respectively. Cells exposed to 30 μM DAM and infected with *C. pneumoniae* for 40 h also exhibited small bacterial vacuoles (green) (E) in contrast to the control unexposed cells (F). Host cells in (E) and (F) are counterstained in red by Evans' blue stain.

Next, the development of infectious *C. trachomatis* L2 EBs was assayed under conditions of iron deficiency. HEp-2 cells, which had been pre-exposed to varying concentrations of DAM, were infected and incubated with DAM for an additional 48 h. Next, cells were homogenized, and the lysate was diluted and subpassaged onto fresh HEp-2 cells for inclusion-forming unit (ifu) and infectivity assessments. As demonstrated in Table 1, chelation of intracellular iron with DAM reduced the number of infectious EBs in a dose-dependent fashion. Taken together, we have observed that, for the growth of *C. trachomatis* L2, limiting iron availability caused the production of generally smaller inclusions, the formation of multiple inclusions that fuse at a later time than normal and a considerable reduction in bacterial infectivity.

Effects of iron chelation on C. pneumoniae *growth*

In experiments with *C. pneumoniae*, we used DAM at concentrations ranging from 5 to 30 μM. Selection of these relatively low concentrations was based on the observation that exposure of the uninfected cells to DAM at concentrations higher than 30 μM for periods longer than 3 days caused detrimental detachment and cell death. DAM concentrations $\leq$ 30 μM did not compromise the viability of cells, as determined by the Trypan blue exclusion test and staining with the fluorescent Mito-Tracker, although sometimes caused minor loss of adherence, depending on the concentration used (data not shown). Based on light microscopy examination, the number of detached cells in infected cultures exposed to 5 or 10 μM DAM was negligible throughout the experimental periods. At DAM concentrations $>$ 10 μM, a dose-dependent increase in detached cells, was noticed 3 days after infection (data not shown).

HEp-2 cells were infected with *C. pneumoniae* and incubated with DAM at 5, 10, 15, 20, 25 or 30 μM. After staining with the appropriate antibodies to visualize bacteria, specimens were analysed by immunofluorescence microscopy. The inclusions in treated cells (Fig. 1E) were smaller than those in control untreated cultures (Fig. 1F). The decrease in inclusion size was dependent on the drug concentration (data not shown).

To test how the lack of iron affects the production of infectious EBs, cells were infected with *C. pneumoniae* in the presence of various DAM concentrations, and the infectivity was assessed at 72 h after infection. The data in Table 1 indicate that the production of infectious

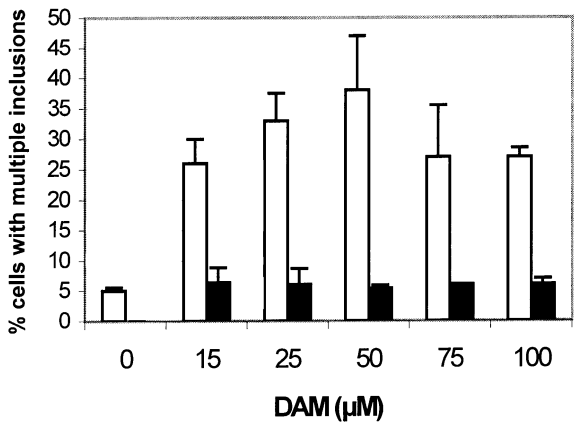

Fig. 2. Restriction of intracellular iron availability delays the homotypic inclusion fusion of *C. trachomatis* L2. Host cells were exposed to various amounts of DAM, infected with *C. trachomatis* at a an MOI of 15:1 and incubated at 37°C for either 20 h (open bars) or 35 h (closed bars). At the indicated time points, inclusions were detected by staining with antichlamydial antibody and FITC-conjugated secondary antibody, and cells with multiple inclusions were counted. The percentage of cells containing multiple inclusions was determined from 100 infected host cells. The data shown represent two independent experiments.

Table 1. Depletion of available free iron significantly reduces the production of infectious progeny of *C. trachomatis* L2 and *C. pneumoniae* in a dose-dependent fashion[a].

	C. trachomatis		*C. pneumoniae*	
DAM (μM)[b]	No. of IFU ml^{-1}[c]	% Infectivity[d]	No. of IFU ml^{-1}[c]	% Infectivity[d]
0	8.32×10^9	100	6.5×10^7	100
5	5.82×10^9	70	6.4×10^6	10
10	4.63×10^9	56	6.2×10^4	0.1
15	4.28×10^8	5	0	0
20	ND	ND	0	0
25	ND	ND	0	0
30	1.19×10^7	0.14	ND	ND
50	5.71×10^5	–	ND	ND
100	3.57×10^4	–	ND	ND

a. The experiments were performed in duplicate.
b. Host cells were preincubated overnight with DAM concentrations ranging from 0 to 100 μM, then infected with *C. trachomatis* L2 (MOI 15:1) or *C. pneumoniae* and incubated for an additional 48 h (*C. trachomatis*) or 72 h (*C. pneumoniae*) in the presence of the respective amounts of DAM.
c. To estimate ifu ml^{-1}, infected cell cultures treated with each DAM concentration were collected, disrupted, serially diluted and inoculated onto fresh HEp-2 cells. Two days after inoculation, inclusions were visualized by immunostaining and counted.
d. The percentage infectivity of *C. trachomatis* L2 or *C. pneumoniae* in each treatment was determined by dividing ifu ml^{-1} estimated for that treatment by ifu ml^{-1} of the control cell cultures (not exposed to DAM) multiplied by 100.
–, Negligible; ND, not done.

progeny was reduced by 5 and 10 μM DAM and totally inhibited at 15–30 μM.

To determine whether the infectivity of chlamydiae grown in the iron-restricted environment can be restored by adding exogenous iron, we used holo-transferrin (HTf) and apo-transferrin (ATf). Cell cultures were first depleted of iron and then infected in the presence of cycloheximide. At specified time points (24, 48 and 72 h after infection), cycloheximide was removed to restore normal protein synthesis by the host cells, and the Tf forms were added (Table 2). Infectivity titres assessed 96 h after initial infection showed that the iron-loaded form of Tf, i.e. HTf, but not ATf, can restore bacterial infectivity in cultures exposed to DAM. HTf reversed the inhibitory effects of DAM when administered 24 h or 48 h after infection (Table 2). In contrast, the effect of HTf was

Table 2. Rescue of infectivity of *C. pneumoniae* grown under iron depletion by exogenous administration of iron-loaded Tf (HTf)[a].

		Time after infection						
	−15 h	0 h	24 h	48 h	72 h	96 h	ifu ml^{-1}	% Infectivity
1	CGM-D	IM + C–D					3.69×10^7	100
2	CGM + D	IM + C–D					3.21×10^7	87
3	CGM + D	IM + C + D					1.40×10^6	4
4	CGM + D	IM–C–D + HTf					3.08×10^7	84
5	CGM + D	IM–C–D + ATf					2.94×10^7	80
6	CGM + D	IM + C + D	IM–C–D				2.65×10^7	72
7	CGM + D	IM + C + D	IM–C + D + HTf				2.20×10^7	60
8	CGM + D	IM + C + D	IM–C + D + ATf				1.57×10^6	4
9	CGM + D	IM + C + D	IM–C–D + HTf				2.59×10^7	70
10	CGM + D	IM + C + D	IM–C–D + ATf				2.81×10^7	76
11	CGM + D	IM + C + D		IM–C–D			1.30×10^7	35
12	CGM + D	IM + C + D		IM–C + D + HTf			1.43×10^7	39
13	CGM + D	IM + C + D		IM–C + D + ATf			1.20×10^6	3
14	CGM + D	IM + C + D		IM–C–D + HTf			1.47×10^7	40
15	CGM + D	IM + C + D		IM–C–D + ATf			1.60×10^7	43
16	CGM + D	IM + C + D			IM–C–D		1.62×10^6	4
17	CGM + D	IM + C + D			IM–C + D + HTf		2.22×10^6	6
18	CGM + D	IM + C + D			IM–C + D + ATf		7.50×10^5	2
19	CGM + D	IM + C + D			IM–C–D + HTf		2.71×10^6	7
20	CGM + D	IM + C + D			IM–C–D + ATf		3.65×10^6	10

a. Host cell cultures preincubated with cell growth medium (CGM) containing 10 μM DAM (D) were infected with *C. pneumoniae*, overlaid with infection medium (IM) containing cycloheximide (C) and DAM and then cultured under standard conditions. At the indicated time points, IM was removed, and fresh medium without C but supplemented with D and either HTf or ATf as indicated was added. At 96 h after infection, all specimens were harvested, and ifu ml^{-1} and percent infectivity were determined for all specimens as described in the legend to Table 1.

minimal when added 72 h after infection for an additional 24 h, a period that is presumably not long enough for significant bacterial binary fission and/or transformation of the RBs into infectious EBs.

To reveal the ultrastructural features of the inclusion and its chlamydial forms, DAM-exposed cell cultures were analysed by electron microscopy. In the treated cells infected for 48 h, small inclusions were present containing mostly RBs (Fig. 3B). The number of bacteria within these inclusions was lower when compared with the untreated controls (Fig. 3A). In addition, electron microscopic ultrathin sections documented a wavy appearance of the chlamydial outer membrane in the cultures deprived of iron (Fig. 3B, arrowhead in the insert) but not in the untreated controls.

Interaction of C. pneumoniae *inclusions with the endocytic pathway of iron-deprived host cells*

In a previous work, we showed that *C. pneumoniae* are confined to inclusions that escape fusion with lysosomes (Al-Younes *et al*., 1999). In addition, we suggested an interaction between inclusions and early endosomes, as TfR was found to be localized adjacent to the inclusions

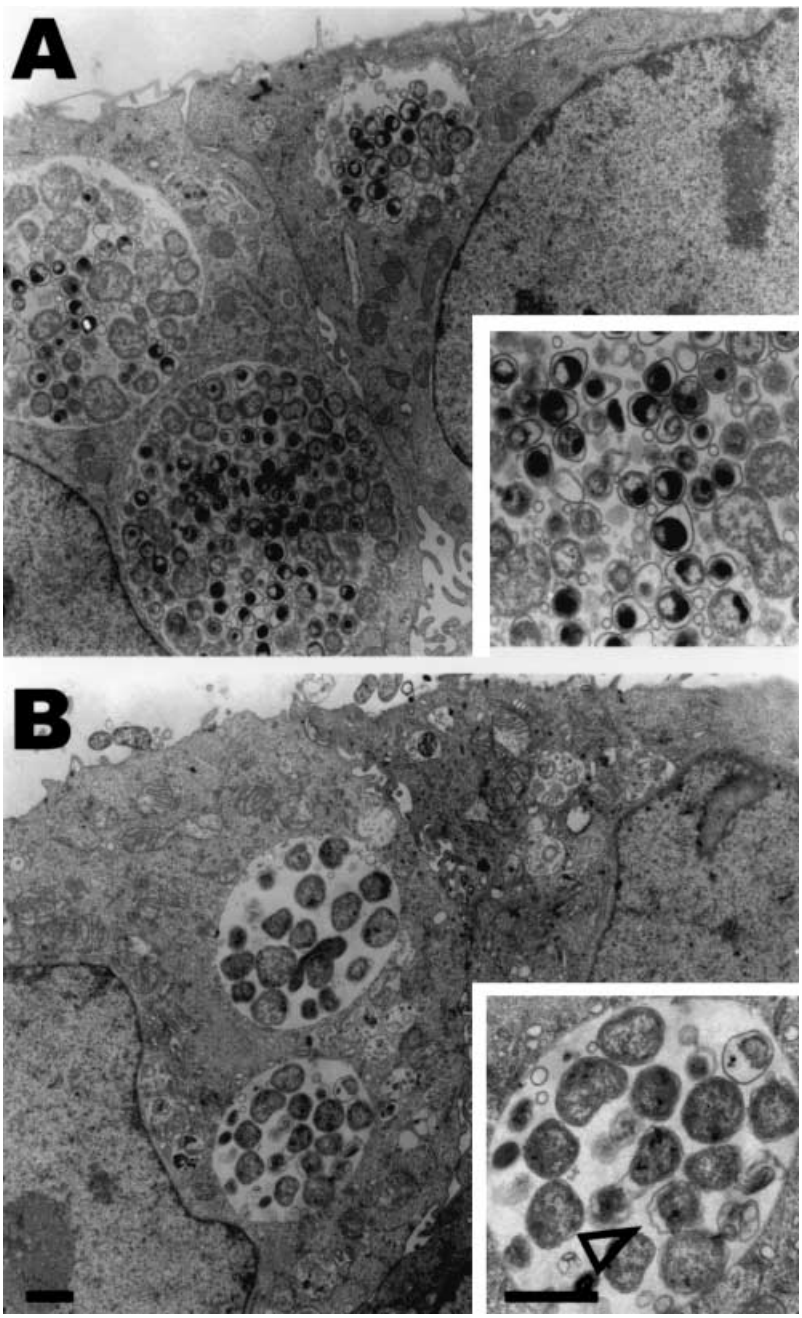

Fig. 3. Transmission electron microscopy showing ultrastructural features of *C. pneumoniae* in infected HEp-2 epithelial cells deprived of iron by exposure to the iron chelator DAM. Host cells were exposed to medium alone or medium containing 30 μM DAM 15 h before infection and throughout the infection period (48 h).
A. Micrograph of infected untreated host cells shows typical inclusions containing all the chlamydial developmental stages.
B. Micrograph of an infected cell exposed to DAM demonstrates the presence of small inclusions that contain fewer chlamydiae, predominantly RBs, compared with the control. High magnification of an inclusion developed in DAM-treated cells reveals a wavy appearance of the bacterial outer membranes (B, arrowhead in the insert). Scale bar represents 1 μm.

(Al-Younes *et al.*, 1999). Here, we examined the interaction of the chlamydial inclusions with vesicles of the endocytic pathway of host cells deprived of iron. Analysis of the confocal microscopy data shows that the inclusions in iron-deprived host cells did not sequester the lysosomal protein marker LAMP-1 (Fig. 4B), similar to those in the control infected cells (Fig. 4A). Interestingly, in the DAM-treated cells, the punctuate pattern of TfR distribution throughout the cytoplasm disappeared, and more abundant accumulation of these receptors was observed surrounding *C. pneumoniae* vacuoles (Fig. 4D and E), unlike in the untreated control (Fig. 4C). These findings were corroborated by electron microscopy using gold immunolabelling, which, in contrast to unexposed cells, showed local concentration of TfR in the vicinity of the inclusion in DAM-exposed cells (data not shown). Surprisingly, gold particles were found in association with small vesicles of unknown origin present either in the lumen of the inclusion or inside compartments located adjacent to the inclusion in the DAM-exposed cells and the unexposed control cells (data not shown). Taken together, these results indicate that limiting the availability of iron does not affect the interaction of the chlamydial inclusions with lysosomes, but increases the amount of TfR attracted to the vicinity of the inclusions.

C. pneumoniae *infection does not affect the amounts of cellular TfR*

To determine whether *C. pneumoniae* infection modifies the expression of TfR by host cells, HEp-2 cells were infected and maintained under standard conditions (in the absence of DAM and cycloheximide). At 0, 6, 21 or 45 h after infection, cellular TfR amounts were analysed by

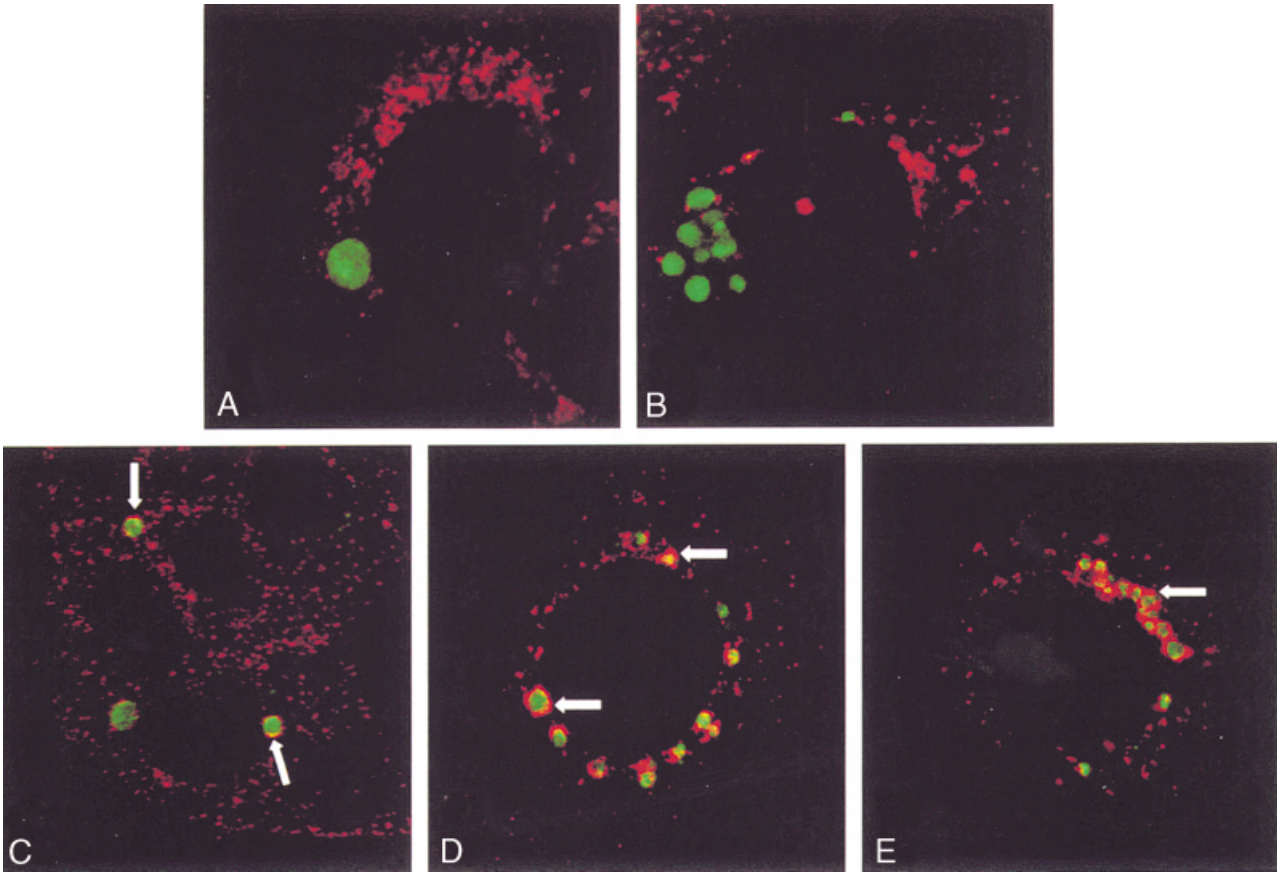

Fig. 4. Double immunofluorescence staining of *C. pneumoniae* and markers of the endocytic system of host cells deprived of iron. HEp-2 cells were exposed to 30 μM DAM, infected with *C. pneumoniae* and incubated at 37°C and 5% CO_2 in the absence of cycloheximide. At 40 h after infection, cells were fixed, permeabilized and stained for *C. pneumoniae* and either the endosomal marker TfR or the lysosomal marker LAMP-1. Chlamydial inclusions (green) in host cells (B) grown in iron-deficient medium do not co-localize with LAMP-1 (red), similar to those in infected cells unexposed to DAM (A).
C. Close association of TfR (arrows, red) with *C. pneumoniae* inclusions normally seen in iron-sufficient control cell cultures.
D and E. Photomicrographs show strong TfR labelling (arrows, red) proximal to chlamydial inclusions in iron-starved host cells. This staining pattern and loss of typical TfR staining in the host cytoplasm reflect specific recruitment of that receptor to the vicinity of inclusions, compared with the control (C).

SDS–PAGE followed by immunoblotting. The total cellular amounts of TfR did not appear to be altered in response to potential changes in intracellular iron level induced by *C. pneumoniae* (data not shown).

Discussion

In this study, we have investigated the role of iron in the growth and development of *C. pneumoniae* in comparison with *C. trachomatis* L2. Restricting the availability of iron in the infected epithelial host cells caused the formation of smaller chlamydial inclusions compared with the infected untreated cells. Infectivity titration experiments showed that *C. pneumoniae* have increased sensitivity to iron deprivation compared with *C. trachomatis* L2. The reduction in infectivity of both species isolated from iron-deprived conditions is primarily attributed to a relatively low number of bacteria present within inclusions that mostly contain the non-infectious RBs, as demonstrated by electron microscopy examination. The inhibitory effect of DAM on *C. pneumoniae* growth was counteracted by the addition of iron-loaded Tf, but not by the iron-free form of Tf. In addition, the characteristic fusion of *C. trachomatis* L2 inclusions within host cells was delayed. The possibility that these effects observed in chlamydial development are the result of compromising host cell viability by DAM has been eliminated by Trypan blue exclusion test and staining of viable mitochondria using the fluorescent dye MitoTracker. However, iron deprivation could affect the host cell metabolism, disturb the usual interaction between host and chlamydiae and indirectly lead to the changes observed in chlamydial development. The lack of a system that would enable the cultivation of free chlamydiae *in vitro* makes the dissection between direct and indirect effects of iron deprivation difficult, if not impossible. Nonetheless, under physiological conditions, the communication between chlamydiae-containing inclusion and extracellular environment will be mediated by a host cell. In summary, our data indicate that iron limitation leads to a delay in chlamydial development and inclusion maturation.

Based on our electron microscopic data, the low number of RBs observed in DAM-exposed cell cultures indicates that iron deprivation resulted in either a delay in or an arresting of division of formed RBs. This pattern of development under iron-deprived conditions was maintained for at least 6 days after infection (electron microscopic data not shown). We speculate that the inhibition of chlamydial cell division demonstrated by electron microscopy and infectivity experiments could be attributed directly to the lack of iron. A number of chlamydial enzymes require iron for their activities. One of them, ribonucleotide reductase, which is probably present in a biochemically active form in *C. trachomatis* (McClarty, 1999), catalyses the reduction of ribonucleotides to their corresponding deoxyribonucleotides, the first step in the pathway leading to DNA synthesis (Reichard, 1988). Iron deprivation could lead to partial or total inhibition of the activity of ribonucleotide reductase, in the end affecting DNA synthesis.

The ability of *Chlamydia* to cause persistent infections is known from the clinical and *in vitro*-derived data. Development of persistence can be induced by cytokines (interferon-γ), antibiotics or by deprivation of some amino acids (Beatty *et al*., 1994). In our experimental model, iron deprivation generated altered development and appearance of chlamydiae, consistent with the findings in persistent infection. Consequently, we hypothesize that changes in iron concentration in the infected tissues or cells could contribute to either long-lasting, atypical chlamydial infection or reactivation of dormant stage infection.

The effects of free iron depletion on *C. psittaci* and the trachoma serovar E of *C. trachomatis* (*C. trachomatis* E) have been investigated previously. Because the number of inclusions in 30 μM DAM-treated and control infected human macrophages were similar, Murray *et al*. (1991) concluded that the intracellular replication of *C. psittaci* is iron independent. Similarly, Raulston (1997) showed no significant differences in the absolute number of *C. trachomatis* E inclusions in DAM (25–100 μM)-exposed and unexposed control HEC-1B epithelial cells. However, it was observed that the use of the iron-specific chelator generated a significant reduction in infectivity of bacteria collected from treated cultures and smaller aberrant inclusions surrounded by electron-dense material containing a lower number of atypical chlamydiae. The bacteria within these inclusions were mostly RBs with dense and wavy outer membranes. In addition, iron limitation enhanced the production of at least 19 chlamydial proteins and restricted the expression of at least one protein, as revealed by two-dimensional PAGE. Our data corroborate the results described earlier for *C. trachomatis* E (Raulston, 1997). However, the two prominent morphological differences appear to be: (i) the lack of electron-dense material in the outer membrane of *C. pneumoniae* RBs and around inclusions developed under iron-limiting conditions; and (ii) the absence of true, profuse blebbing within *C. pneumoniae* inclusions, potentially reflecting differences in the concentration of iron chelator, chlamydial species and the host cells used. Furthermore, in the experiments with *C. trachomatis* L2, we have observed a delay in the homotypic fusion of the inclusions upon iron deprivation. This delay, detected in *C. trachomatis* L2, a representative of the LGV biovar, but not in *C. trachomatis* E, which belongs to the trachoma biovar, could reflect biological and pathological differences between these biovars. Although both biovars exhibit almost 100% DNA homology, they differ in their infectivity *in vivo* and *in vitro* (Chen and Stephens, 1997).

Furthermore, the *C. trachomatis* LGV biovar that infects lymphatic cells is invasive in nature, whereas the trachoma biovar remains non-invasive and localized to the epithelium of ocular tissue and the urogenital tract (Raulston, 1995).

Microorganisms obtain the iron required for their metabolic activities using different mechanisms. Some bacteria, such as *Mycobacterium* (De Voss *et al*., 1999), *Yersinia pestis* (Perry *et al*., 1999), *Escherichia coli* and *Pseudomonas aeruginosa* (Vartivarian and Cowart, 1999), produce siderophores, soluble iron-chelating compounds that are able to mobilize iron from high-affinity iron-binding compounds such as Tf. Other bacteria, such as *Neisseria*, *Haemophilus* (Cornelissen and Sparling, 1994) and *Moraxella* (Luke and Campagnari, 1999), express their own receptors for Tf. Iron uptake by intracellular pathogens may be facilitated by residing in an early endosomal compartment that selectively accumulates TfR such as *Ehrlichia* (Barnewall *et al*., 1999) and/or by upregulating TfR expression within infected cells such as *Coxiella burnetii* (Howe and Mallavia, 1999).

The mechanism(s) of iron delivery to *Chlamydia* is still unclear. Homologues for bacterial siderophores or their receptors are missing in the *C. pneumoniae* and *C. trachomatis* genomes (Stephens, 1999). In addition, TfR expression does not appear to be modulated by *Chlamydia* infection (this study; Scidmore *et al*., 1996). However, the redistribution of Tf and TfR in close apposition to inclusions when chlamydiae are grown in iron-sufficient medium (Scidmore *et al*., 1996; Taraska *et al*., 1996; Van Ooij *et al*., 1997; Hackstadt *et al*., 1998; Al-Younes *et al*., 1999) may be part of a novel pathway of iron acquisition by these bacteria. This notion is supported by the enhanced recruitment of these receptors, shown in this study, around inclusions when *Chlamydia* are grown in iron-deficient medium, possibly reflecting the needs of the organism for that essential element.

In summary, our data, together with those reported by Raulston (1997), suggest that iron deprivation causes a delay in chlamydial maturation and that *Chlamydia* may access and use the free iron pool or Tf of host cells. We also postulate that iron limitation does not inhibit invasion, the formation of inclusions and differentiation of invading EBs into RBs in host cells, but could affect RB binary fission and subsequent transition of developed RBs to EBs. The altered maturation of chlamydiae described in our experimental system suggests that the low iron level could be a factor playing a role in the induction of persistent infections.

Experimental procedures

Media and reagents

Cell growth medium (CGM) consisted of minimal essential medium containing Earle's salts (Gibco BRL) supplemented with 1% non-essential amino acids (Sigma), 2 mM L-glutamine (Biochrom), 10% fetal bovine serum (FBS), 10 mM HEPES (Sigma) and 10 μg ml^{-1} gentamicin. Infection medium (IM) consisted of the same components as CGM with only 5% FBS and 1 μg ml^{-1} cycloheximide (Sigma), a drug that reversibly inhibits host cell protein synthesis.

The iron-chelating agent deferoxamine mesylate (DAM), Moviol mounting medium, glutaraldehyde and DL-dithiothreitol (DDT) were obtained from Sigma. Holo-transferrin (HTf; iron-loaded form of Tf) and apo-Tf (ATf; iron-free form of Tf) were purchased from Calbiochem. Paraformaldehyde (PFA) and Triton X-100 were from Merck. Bovine serum albumin (BSA), sodium dodecyl sulphate (SDS) and bromophenol blue were obtained from Biomol. Sucrose, Tris-HCl and glycerol were from Roth. Agar 100 was from Agar Scientific.

Eukaryotic host cells

The host cell lines used in this study were the human epithelial HEp-2 (ATCC-CCL23) derived from a laryngeal carcinoma and HeLa (ATCC-CCL2.1), which originated from a cervix carcinoma. Host cells were grown in CGM using standard conditions (37°C and 5% CO_2 in a humidified tissue culture incubator).

Bacteria and their propagation

C. pneumoniae strain TW-183 was obtained from the Washington Research Foundation, and *C. trachomatis* serovar L2 was a gift from Dr H. Brade, Center for Medicine and Biosciences, Borstel, Germany. *C. pneumoniae* propagation, subsequent isolation from infected cells and infectivity titration were performed as described earlier (Al-Younes *et al*., 1999). For the experimental infections, the bacterial dilution able to infect at least 60–70% of host cells in monolayers was used. *C. trachomatis* L2 EBs were harvested from HeLa cells grown in 175 cm^2 culture flasks and infected for 48–72 h. For the assessment of infectivity titre, HeLa cells were inoculated with purified, serially diluted EBs, and the number of inclusion-forming units (ifu) ml^{-1} was calculated.

Manipulation of the host intracellular iron levels and the Chlamydia *infection assays*

Iron depletion experiments. To study the effect of iron chelation on *C. pneumoniae* growth, HEp-2 cells were cultured in CGM in 12-well plates with or without 13-mm-diameter coverslips and exposed overnight to various concentrations (0, 5, 10, 15, 20, 25 and 30 μM) of DAM. On the following day, host cells were infected using the previously established *C. pneumoniae* dilution able to infect at least 60–70% of cells, with the aid of centrifugation (900 *g* at 35°C for 1 h), with freshly thawed *C. pneumoniae* EBs diluted in IM containing the respective amounts of DAM and then incubated for an additional 1 h in 5% CO_2 at 37°C. After two washes, fresh IM containing the respective DAM concentrations was added, and the plates were incubated further for specified times. To reduce the rate of iron uptake

by infected cells, TfR synthesis was suppressed by including cycloheximide in IM as described by Raulston (1997). The developmental and growth features of the bacteria were examined by staining cell cultures grown on coverslips 48 h after infection with the suitable antibodies followed by immunofluorescence microscopy. To assess the influence of iron deprivation on *C. pneumoniae* infectivity, infected cells cultured in plates were harvested 72 h after infection, homogenized, serially diluted and subpassaged onto HEp-2 cells grown on coverslips. Two days after infection, chlamydial inclusions were visualized by immunostaining and counted to determine the ifu ml^{-1}.

To explore the effects of iron deficiency on *C. trachomatis* L2, HEp-2 cells seeded in 12-well plates were preincubated overnight in CGM with 0, 5, 10, 15, 30, 50 or 100 μM DAM and then infected with *C. trachomatis* L2 at a 15:1 MOI. Bacteria were diluted in IM containing the respective amounts of DAM and allowed to adsorb to host cells for 2 h in 5% CO_2 at 37°C. Next, monolayers were washed and incubated for 48 h in fresh IM plus DAM. Cells were then lysed, serially diluted and the infectivity of bacteria was determined. The effects of DAM on the morphology and size of *C. trachomatis* L2 inclusions were investigated using phase-contrast and immunofluorescence microscopy.

Influence of HTf on C. pneumoniae growth. To confirm that DAM-mediated inhibition of *C. pneumoniae* growth was caused by iron starvation of the bacteria, infected cells were exposed to either exogenous HTf or ATf according to the method of Raulston (1997) with modifications. Briefly, HEp-2 cells were grown overnight in CGM with 10 μM DAM. After infection with *C. pneumoniae*, cells were overlaid with IM with or without 10 μM DAM and incubated in 5% CO_2 at 37°C. At either 24, 48 or 72 h after infection, fresh IM without cycloheximide and with DAM and either 0.4 mg ml^{-1} HTf (final concentration) or 0.4 mg ml^{-1} ATf (final concentration) (Table 2) was added to abrogate the inhibitory effects of DAM. At 96 h after infection, all specimens were harvested, homogenized and inoculated onto fresh HEp-2 cells to estimate the chlamydial infectivity titre (ifu ml^{-1}).

Host cell viability

Monolayers of HEp-2 cells were exposed to DAM concentrations ranging from either 5 to 100 μM for 48 h or 5 to 30 μM for 72 h and incubated under similar conditions to those described in the infection experiments. Other cell monolayers were incubated with 0.4 mg ml^{-1} HTf or ATf (final concentration) for 72 h. The cultures were then assayed for viability using two methods: the Trypan blue exclusion test and staining with the cationic fluorescent dye MitoTracker orange CMTMRos (MitoTracker) (Molecular Probes). The latter method assesses viability by detecting the presence of a transmembrane potential across the mitochondrial membrane.

Antibodies and immunofluorescence labelling

For the detection of *C. pneumoniae* within infected host cells, a mouse monoclonal species-specific antibody directly coupled with fluorescein isothiocyanate (FITC) was used as recommended by the manufacturer (Imagen kit; Dako). To visualize *C. trachomatis* inclusions, monolayers of infected cells were washed with PBS (pH 7.4) and fixed for 30 min with 4% PFA−120 mM sucrose in PBS, pH 7.4. Next, the cells were permeabilized with 0.2% Triton X-100–0.2% BSA in PBS for 30 min at room temperature, followed by incubation with rabbit polyclonal genus-specific antichlamydial antibody (Milan Analytica) for 1 h. After three washes with PBS, specimens were stained for 1 h with FITC-coupled goat anti-rabbit IgG (Jackson ImmunoResearch Laboratories), washed, air dried and mounted with Moviol mounting medium. Slides were examined using a Leica conventional immunofluorescence microscope.

For the dual staining of *C. pneumoniae* and either the endosomal marker TfR or the lysosomal marker LAMP-1 (lysosomal-associated membrane protein-1), cell cultures were fixed and permeabilized as described above. The specimens were then labelled with the rabbit polyclonal *Chlamydia*-specific antibody and either mouse monoclonal anti-human TfR (Dako) or LAMP-1 antibody (Developmental Studies Hybridoma Bank, University of Iowa, IA, USA). For the detection, FITC-conjugated goat anti-rabbit and rhodamine-conjugated goat anti-mouse antibodies (Jackson ImmunoResearch Laboratories) were used. Double-stained specimens were then analysed with a Leica TCS NT laser-scanning confocal microscope.

Transmission electron microscopy (TEM)

To analyse the ultrastructural features of *C. pneumoniae* grown under iron-deficient conditions, infected host cells were fixed with 2.5% glutaraldehyde, post-fixed with 1% OsO_4 and then contrasted with tannic acid and uranyl acetate. The specimens were dehydrated in a graded ethanol series and embedded in Agar 100. Ultrathin sections were contrasted with lead citrate and examined with a Zeiss EM 10 electron microscope.

SDS–PAGE and immunoblotting

At the indicated time points, cells were detached by gentle shaking with sterile 3-mm-diameter glass beads and frozen in aliquots of 1×10^5 cells 50 μl^{-1} of PBS at −20°C. Before electrophoresis, the samples were denatured in an equal volume of 2× SDS lysis buffer (100 mM Tris-HCl, pH 6.8, 4% SDS, 20% glycerol, 0.2% bromophenol blue, 0.2 M DDT). Ten microlitres of each sample (1×10^4 cells) was resolved on 8% polyacrylamide gels and transferred electrophoretically onto Immobilon-P polyvinylidene difluoride (PVDF) membranes (Millipore). The membranes were blocked with 3% BSA in TBS (Tris-buffered saline, pH 7.5) and incubated with mouse monoclonal anti-human TfR antibody (1:1000; Zymed Laboratories). The washed membranes were then incubated with goat anti-mouse IgG directly conjugated with horseradish peroxidase (Amersham) diluted 1:2000. Signal detection was performed with the enhanced chemiluminescence system (ECL; Amersham).

Acknowledgements

This work was supported in part by the Fonds der Chemische Industrie. H.M.A. gratefully acknowledges receipt of a PhD fellowship from the Deutscher Akademischer Austauschdienst (DAAD).

References

Al-Younes, H.M., Rudel, T., and Meyer, T.F. (1999) Characterization and intracellular trafficking pattern of vacuoles containing *Chlamydia pneumoniae* in human epithelial cells. *Cell Microbiol* **1**: 237–247.

Barnewall, R.E., and Rikihisa, Y. (1994) Abrogation of gamma interferon-induced inhibition of *Ehrlichia chaffeensis* infection in human monocytes with iron-transferrin. *Infect Immun* **62**: 4804–4810.

Barnewall, R.E., Ohashi, N., and Rikihisa, Y. (1999) *Ehrlichia chaffeensis* and *E. sennetsu*, but not the human granulocytic ehrlichiosis agent, colocalize with transferrin receptor and up-regulate transferrin receptor mRNA by activating iron-responsive protein. *Infect Immun* **67**: 2258–2265.

Beatty, W.L., Morrison, R.P., and Byrne, G.I. (1994) Persistent chlamydiae: from cell culture to a paradigm for chlamydial pathogenesis. *Microbiol Rev* **58**: 686–699.

Blyth, W.A., and Taverne, J. (1972) Some consequences of the multiple infection of cell cultures by TRIC organisms. *J Hyg (London)* **70**: 33–37.

de Boer, O.J., van der Wal, A.C., and Becker, A.E. (2000) Atherosclerosis, inflammation, and infection. *J Pathol* **190**: 237–243.

Byrd, T.F., and Horwitz, M.A. (1989) Interferon gamma-activated human monocytes downregulate transferrin receptors and inhibit the intracellular multiplication of *Legionella pneumophila* by limiting the availability of iron. *J Clin Invest* **83**: 1457–1465.

Cabantchik, Z.I., Moody-Haupt, S., and Gordeuk, V.R. (1999) Iron chelators as anti-infectives; malaria as a paradigm. *FEMS Immunol Med Microbiol* **26**: 289–298.

Chen, J.C., and Stephens, R.S. (1997) *Chlamydia trachomatis* glycosaminoglycan-dependent and independent attachment to eukaryotic cells. *Microb Pathog* **22**: 23–30.

Cornelissen, C.N., and Sparling, P.F. (1994) Iron piracy: acquisition of transferrin-bound iron by bacterial pathogens. *Mol Microbiol* **14**: 843–850.

De Voss, J.J., Rutter, K., Schroeder, B.G., and Barry, C.E., III (1999) Iron acquisition and metabolism by mycobacteria. *J Bacteriol* **181**: 4443–4451.

Fortier, A.H., Leiby, D.A., Narayanan, R.B., Asafoadjei, E., Crawford, R.M., Nacy, C.A., and Meltzer, M.S. (1995) Growth of *Francisella tularensis* LVS in macrophages: the acidic intracellular compartment provides essential iron required for growth. *Infect Immun* **63**: 1478–1483.

Grayston, J.T., Campbell, L.A., Kuo, C.C., Mordhorst, C.H., Saikku, P., Thom, D.H., and Wang, S.P. (1990) A. new respiratory tract pathogen: *Chlamydia pneumoniae* strain TWAR. *J Infect Dis* **161**: 618–625.

Hackstadt, T., Scidmore-Carlson, M.A., and Fisher, E.R. (1998) Rapid dissociation of the *Chlamydia trachomatis* inclusion from endocytic compartments. In *Proceedings of the 9th International Symposium on Human Chlamydial Infections.* Stephens, R.S., Byrne, G.I., Christiansen, G., Clark, I.N., Grayston, J.T., Rank, R.G. *et al.* (eds). University of California, Berkeley Press, pp. 127–130.

Hackstadt, T., Scidmore-Carlson, M.A., Shaw, E.I., and Fisher, E.R. (1999) The *Chlamydia trachomatis* IncA protein is required for homotypic vesicle fusion. *Cell Microbiol* **1**: 119–130.

Howe, D., and Mallavia, L.P. (1999) *Coxiella burnetii* infection increases transferrin receptors on J774A. 1 cells. *Infect Immun* **67**: 3236–3241.

Jacobs, A. (1977) Low molecular weight intracellular iron transport compounds. *Blood* **50**: 433–439.

Luke, N.R., and Campagnari, A.A. (1999) Construction and characterization of *Moraxella catarrhalis* mutants defective in expression of transferrin receptors. *Infect Immun* **67**: 5815–5819.

McClarty, G. (1999) Chlamydial metabolism as inferred from the complete genome sequence. In *Chlamydia: Intracellular Biology, Pathogenesis and Immunity.* Stephens, R.S. (ed.). Washington, DC: American Society for Microbiology Press, pp. 69–100.

Matsumoto, A., Bessho, H., Uehira, K., and Suda, T. (1991) Morphological studies of the association of mitochondria with chlamydial inclusions and the fusion of chlamydial inclusions. *J Electron Microsc (Tokyo)* **40**: 356–363.

Murray, H.W., Granger, A.M., and Teitelbaum, R.F. (1991) Gamma interferon-activated human macrophages and *Toxoplasma gondii*, *Chlamydia psittaci*, and *Leishmania donovani*: antimicrobial role of limiting intracellular iron. *Infect Immun* **59**: 4684–4686.

Peeling, R.W., and Brunham, R.C. (1996) Chlamydiae as pathogens: new species and new issues. *Emerg Infect Dis* **2**: 307–319.

Perry, R.D., Balbo, P.B., Jones, H.A., Fetherston, J.D., and DeMoll, E. (1999) Yersiniabactin from *Yersinia pestis*: biochemical characterization of the siderophore and its role in iron transport and regulation. *Microbiology* **145**: 1181–1190.

Ponka, P. (1999) Cellular iron metabolism. *Kidney Int Suppl* **69**: S2–S11.

Ponka, P., and Lok, C.N. (1999) The transferrin receptor: role in health and disease. *Int J Biochem Cell Biol* **31**: 1111–1137.

Ramirez, J.A. (1996) Isolation of *Chlamydia pneumoniae* from the coronary artery of a patient with coronary atherosclerosis. The *Chlamydia pneumoniae*/Atherosclerosis Study Group. *Ann Intern Med* **125**: 979–982.

Raulston, J.E. (1995) Chlamydial envelope components and pathogen–host cell interactions. *Mol Microbiol* **15**: 607–616.

Raulston, J.E. (1997) Response of *Chlamydia trachomatis* serovar E to iron restriction *in vitro* and evidence for iron-regulated chlamydial proteins. *Infect Immun* **65**: 4539–4547.

Reichard, P. (1988) Interactions between deoxyribonucleotide and DNA synthesis. *Annu Rev Biochem* **57**: 349–374.

Saikku, P. (2000) Epidemiologic association of *Chlamydia pneumoniae* and atherosclerosis: the initial serologic observation and more. *J Infect Dis* **181** (Suppl. 3): S411–S413.

Scidmore, M.A., and Hackstadt, T. (1995) Ability of *Chlamydia trachomatis* to obtain iron from transferrin. In *Abstracts of the 95th General Meeting of the American Society to Microbiology*, p. 277. Washington DC: American Society for Microbiology.

Stephens, R.S. (1999) Genomic autobiographies of chlamydiae. In *Chlamydia: Intracellular Biology, Pathogenesis and Immunity.* Stephens, R.S. (ed.). Washington, DC: American Society for Microbiology Press, pp. 9–28.

Sullivan, J.L. and Weinberg, E.D. (1999) Iron and the role of *Chlamydia pneumoniae* in heart disease *Emerg Infect Dis* **5**: 724–726.

Taraska, T., Ward, D.M., Ajioka, R.S., Wyrick, P.B., Davis-

Kaplan, S.R., Davis, C.H., and Kaplan, J. (1996) The late chlamydial inclusion membrane is not derived from the endocytic pathway and is relatively deficient in host proteins. *Infect Immun* **64**: 3713–3727.

Van Ooij, C., Apodaca, G., and Engel, J. (1997) Characterization of the *Chlamydia trachomatis* vacuole and its interaction with the host endocytic pathway in HeLa cells. *Infect Immun* **65**: 758–766.

Van Ooij, C., Homola, E., Kincaid, E., and Engel, J. (1998) Fusion of *Chlamydia trachomatis*-containing inclusions is inhibited at low temperatures and requires bacterial protein synthesis. *Infect Immun* **66**: 5364–5371.

Vartivarian, S.E., and Cowart, R.E. (1999) Extracellular iron reductases: identification of a new class of enzymes by siderophore-producing microorganisms. *Arch Biochem Biophys* **364**: 75–82.